

**Please cite the Published Version**

Gao, Zhaohe, Zhang, Xun, Cao, Sheng, Kulczyk-Malecka, Justyna , Qin, Shiyong, Liu, Xiaodong, Kelly, Peter , Wu, Xinhua, Xiao, Ping and Chiu, Yu-Lung (2023) A protective SiAlN coating on topographic surface of laser powder bed fusion manufactured Ti alloy. *Corrosion Science*, 219. p. 111250. ISSN 0010-938X

**DOI:** <https://doi.org/10.1016/j.corsci.2023.111250>

**Publisher:** Elsevier

**Version:** Accepted Version

**Downloaded from:** <https://e-space.mmu.ac.uk/631978/>

**Usage rights:**  [Creative Commons: Attribution-Noncommercial-No Derivative Works 4.0](https://creativecommons.org/licenses/by-nc-nd/4.0/)

**Additional Information:** This is an Accepted Manuscript of an article which appeared in final form in *Corrosion Science*, published by Elsevier

**Data Access Statement:** Data will be made available on request.

**Enquiries:**

If you have questions about this document, contact [openresearch@mmu.ac.uk](mailto:openresearch@mmu.ac.uk). Please include the URL of the record in e-space. If you believe that your, or a third party's rights have been compromised through this document please see our Take Down policy (available from <https://www.mmu.ac.uk/library/using-the-library/policies-and-guidelines>)

# A protective SiAlN coating on topographic surface of laser powder bed fusion manufactured Ti alloy

Zhaohe Gao<sup>a,b,\*</sup>, Xun Zhang<sup>a</sup>, Sheng Cao<sup>a</sup>, Justyna Kulczyk-Malecka<sup>c</sup>, Shiyong Qin<sup>a</sup>, Xiaodong Liu<sup>a</sup>, Peter Kelly<sup>c</sup>, Xinhua Wu<sup>d</sup>, Ping Xiao<sup>a\*</sup> and Yu-Lung Chiu<sup>b\*</sup>

<sup>a</sup>Henry Royce Institute, Department of Materials, University of Manchester, Manchester, M13 9PL, UK

<sup>b</sup>School of Metallurgy & Materials, University of Birmingham, Birmingham, B15 2TT, UK

<sup>c</sup>Surface Engineering Group, Manchester Metropolitan University, Manchester, M1 5GD, UK

<sup>d</sup>Department of Materials Science and Engineering, Monash University, VIC 3800, Australia

## Abstract

Protective SiAlN coating with Mo interlayer has been directly deposited onto as-built topographic surface of laser-based powder bed fusion manufactured Ti6Al4V alloy where high surface roughness, even with irregular geometrical features and native oxide scale on it. The topographic surface of Ti6Al4V is well protected by SiAlN/Mo coatings without spallation, cracks or even oxidation after 50 h of exposure at 800°C for 10 cycles in air. The conformal nature of sputtered SiAlN/Mo coatings enables topographic surface to be well covered, and Mo diffuses through thin native oxide scale on topographic surface into Ti alloy, thereby forming strong chemical bonding between coatings and Ti substrates.

**Keywords:** SiAlN coating; Topographic surface; Laser powder bed fusion; Oxidation protection; Chemical bonding; Magnetron sputtering

## 1. Introduction

Ti and Ti alloys have increasingly been applied in the aeroengine gas turbines (e.g. fan blades, compressors, etc.), medical plants, power generation, chemical and automotive industries owing to their specific strength, superior mechanical properties at elevated temperatures, low density, and outstanding corrosion resistance [1-6]. Laser-based powder bed fusion (L-PBF), is an additive manufacturing (AM) technique, which enables the manufacturing of complex geometries of Ti alloys that consist of complex features not possible to produce with conventional manufacturing techniques (e.g. casting, forging, etc.) [2, 7-12]. Compared with the high cost of producing Ti alloys via conventional techniques, L-PBF also has an economic impact owing to its short production runs and its advantage in reducing material wastage as it only needs raw powder for building the components with limited

machining [13-16]. However, regardless of the manufacturing technique, Ti alloys have inadequate oxidation resistance upon elevated temperatures (especially above 500°C) owing to the limited protection offered by the native oxide scale, thereby restricting its suitability for use in fuel-efficient innovations in aeroengines where the components (e.g. compressor) are increasingly exposed to relatively higher temperature [17]. In order for Ti alloys to be safely applied at higher temperature, coating technology is a particularly attractive path to improve the oxidation resistance.

It is well known that a protective coating design for a metallic substrate against thermal exposure at high temperature mainly consists of a top thermally stable thin film and good coating-substrate integrity (complete coverage, no spallation and no cracks). Amorphous nanocomposite SiMeN ( $\text{Si}_3\text{N}_4/\text{MeN}$ , Me=Al, Ti, Zr, Cr) coatings displaying good thermal stability and excellent oxidation resistance in air at high temperatures have been manufactured by Physical Vapour Deposition (PVD) via magnetron sputtering and can be a promising candidate for the top protective layer [17-19]. Sputtering deposition is a process in which energetic particles (atoms, ions, and clusters) originating at the target surface are ejected from the target and subsequently deposit onto a substrate to form a film [20]. Generally, substrates used for sputter coating need pre-treatment (e.g. machining) to improve the surface quality of the substrate, thereby acquiring a strong interfacial bonding between coating and substrate [21]. The surface quality depends on the following factors: 1) impurities on the surface (oxide scale, foreign particle/contaminant); 2) presence of voids or pits; 3) surface roughness; 4) surface morphology [20, 21]. Generally, the as-built surfaces of L-PBF manufactured alloys have high surface roughness and present some irregular geometrical features on it in comparison with conventionally machined parts [7, 15, 22-25]. The as-fabricated surface quality of a L-PBF manufactured alloy is influenced by the manufacturing parameters, e.g. laser beam power, spot size, scanning speed, hatching distance, layer thickness, etc., and the scanning strategies, e.g. contour scanning, skywriting scanning, etc [7, 13, 26-31]. Decreasing the energy density of the laser beam along with increasing scanning speed has gradually given rise to a rougher surface in L-PBF manufactured Ti alloys [7]. Spattered particles can be produced, which stick on the top surface of the printed alloys under relatively low energy density and fast scanning speeds [32]. These conditions can cause high viscosity and fast cooling rate of the melt pool and the molten metal lacks enough driving force and time to spread, thereby causing the formation of a wavy surface on top of L-PBF manufactured alloys. Moreover, the rippled morphology on the top surface forms by shear force due to the surface tension of the liquid melt pool, which is influenced by the motion of the laser beam [33, 34]. The surface quality of as-built alloys varies with location, e.g. top surface, inclined surface, and bottom surface [13, 15]. A small number of open or closed cavities, partially melted metal powders, irregular geometrical features, and balling effect are more likely to be formed on inclined surfaces (e.g.

side surfaces) [13]. Therefore, considering the relatively poor surface quality of as-built L-PBF manufactured alloys, it is hard to propose a PVD sputtering coating directly deposits on the topographic surface with a small number of imperfections and irregular geometrical features on it of the as-built L-PBF manufactured alloys. Also, it is rare for a metallic substrate to have no surface pre-treatment prior to the deposition of sputtered coatings. However, the long-term goal for additive manufacturing is to produce a product where no post-processing machine finishing is required, which currently has not yet been achieved. Therefore, it is worthwhile exploring the potential of a protective PVD coating directly deposited on the as-fabricated additive manufactured alloys, which enables the AMed products to be net-shape and to facilitate versatile functionality.

In this study, we have directly deposited 0.9  $\mu\text{m}$  thick SiAlN coating with a Mo interlayer on the as-built surfaces (top surface and inclined surface) of L-PBF manufactured Ti6Al4V alloys and the ground surface of Ti6Al4V alloys by magnetron sputtering. The effect of different surface qualities on the bonding and oxidation protection of the SiAlN/Mo coatings at scales from macro to nano have been examined via X-ray  $\mu$ -CT to transmission electron microscopy (TEM). This work provides new insights into that which kind of as-built surfaces of a L-PBF manufactured Ti alloy can combine well with a PVD coating.

## 2. Experiments and Methods

### 2.1 L-PBF manufactured alloys and PVD coating

The 0.9  $\mu\text{m}$  thick SiAlN coatings with Mo interlayer were deposited on the as-built surfaces (top surface and inclined surface) of L-PBF manufactured Ti6Al4V (wt. %) alloys and the ground surface of Ti6Al4V alloys by magnetron sputtering. The L-PBF manufactured Ti6Al4V alloys were built by an EOS M280 machine under a 99.99% Ar protective atmosphere, using the spherical Ti6Al4V powders (6.14%Al, 4.13V, 0.008C, 0.03N, 0.001H, 0.09Fe, wt.%) with a diameter of up to 63  $\mu\text{m}$ . The laser power, laser spot size, and scanning speed were 280 W, 0.1 mm, and 1200 mm/s, respectively. The layer thickness and hatch distance of the built samples were 30  $\mu\text{m}$  and 140  $\mu\text{m}$ , respectively. The scanning direction was altered by 66.6° against the previous scanned layer, more details are shown in our previous work [35]. The printed samples were also annealed at 800°C for 2 h in a vacuum furnace. The oxygen concentrations in the raw powders and annealed L-PBF manufactured samples were measured and oxygen pick-up was 165 ppm during L-PBF process and following vacuum annealing. As for the geometry of the L-PBF manufactured samples, the cross-section of samples was hexagonal and the lengths of the side were  $\sim$ 0.6 cm, as shown in Supplementary Fig.S1. The L-PBF manufactured samples were cut along the black dashed line using a SiC blade in a precision cut-off machine (Accuton 5,

Struers) and the upper half of the L-PBF manufactured samples were acquired, as shown in Fig.1. The upper parts were cleaned by soapy water and acetone (ultrasonic bath for 5 minutes), and then were directly used as the substrates for PVD coating deposition. As for the ground Ti6Al4V substrates, the printed rods were sectioned along the cross-sections perpendicular to the length direction using a SiC blade, acquiring ~0.4 cm thick plates. The plates were ground by SiC abrasive papers from Grit size P400 (Metprep) to P800 and finally P1200, and were then cleaned as before for PVD coating deposition.

The SiAlN/Mo deposition was carried out by reactive magnetron sputtering in a Teer Coatings UDP 350 system. Three vertically opposed unbalanced magnetrons (100 mm × 300 mm<sup>2</sup>) were installed through the chamber walls. An unheated substrate holder (metallic plate) was installed in the centre of the chamber and could rotate at different speeds. The 99.95% pure Si, Al, and Mo targets (300 × 100 mm<sup>2</sup>) were fitted onto the unbalanced magnetrons. The as-fabricated and ground L-PBF manufactured Ti6Al4V alloys were fixed to the substrate holder and the top surface of the as-built L-PBF manufactured alloys was facing the targets. The chamber was pumped to a pressure of lower than  $1.0 \times 10^{-3}$  Pa. Prior to the SiAlN/Mo coating deposition, the substrates were sputter cleaned by Ar<sup>+</sup> ions for 15 minutes by applying a bias of -600 V on the substrate holder in a pure Ar atmosphere. Then, the deposition of the Mo interlayer was carried out in an Ar-only atmosphere; the Mo target was powered by a pulsed DC power supply (Advanced Energy Pinnacle Plus, 500 W, 100 KHz, 50 % duty). Finally, the deposition of SiAlN was carried out in an Ar and N<sub>2</sub> environment, and the Si and Al targets were powered at 700 W and 300 W, respectively. The flow rates of Ar and N<sub>2</sub> during bias cleaning, Mo deposition and SiAlN deposition were controlled by mass flow controllers and the partial pressure of chamber was constantly monitored, as described in detail in previous work [36]. A DC bias of -30 V was applied to the sample holder during Mo deposition (~20 minutes) and SiAlN deposition (~120 minutes), and the holder was rotated at a speed of 5 rpm.

## 2.2 Oxidation test and characterisation

The SiAlN/Mo coated coupons were sectioned into smaller pieces using a SiC cutting blade and the samples were cleaned with soapy water. For the cyclic oxidation test, the coated samples were thermally exposed at 800°C for 5 h in the air in a CM<sup>TM</sup> furnace with a heating rate of 100°C/ minute and then with the sample stage retracted out of the hot zone, cooled by forced air for 10 minutes, then returned for the next cycle.

The top surfaces and cross-sections of the as-fabricated and thermal exposed SiAlN/Mo coated coupons were analysed by scanning electron microscopy (SEM, FEI, Quanta 650, TESCAN), coupled with a focused ion beam (FEI, Helios 660, Xe plasma FIB ). To investigate the microstructure and

elemental composition in detail, thin lamellae were prepared by a FIB via lift-out technique and then investigated by a transmission electron microscopy (TEM, FEI, Talos F200) fitted with the Super - X-EDS system. In order to track the features in 3D virtualisation and at a macro length scale, an X-ray  $\mu$ -CT scan (Nikon XTEK XTH-225) was applied to acquire X-ray tomographs of as-deposited and thermal exposed coated coupons.

### 3. Results

#### 3.1 As-deposited SiAlN/Mo coating on L-PBF manufactured Ti6Al4V

The SiAlN/Mo coatings have been directly deposited on the originally topographic surface of L-PBF manufactured Ti6Al4V alloy samples and the ground flat surface of Ti6Al4V alloy samples. Fig.1 shows the X-ray  $\mu$ -CT 3D volume and SEM micrographs of an as-deposited SiAlN/Mo coating on the topographic surface of the L-PBF manufactured Ti6Al4V alloy. The backscattered electron images in Fig.1 b, c, and d, indicate complete coverage of the SiAlN/Mo coatings on both the top topographic surface and inclined (side) surface. Fig. 1 d displays that the unmelted spherical particles on the side surface have also been well protected by the coatings. The boundaries among different laser scanning on the top topographic surface have consistently been covered by the SiAlN/Mo coatings, as shown in Fig.1 b and Fig.2 a. Fig.2 b and c show the cross-sectional SEM and high-angle annular dark-field (HAADF) images of the SiAlN/Mo coating on the top surface of the L-PBF manufactured Ti6Al4V. The SiAlN coating shows a smooth, dense, and homogeneous microstructure without any signs of defects, as shown in Fig.2 b and c. The Mo interlayer deposited between the Ti6Al4V and SiAlN, provides a bonding role between the SiAlN coating and the Ti alloy substrate. Fig.2 d shows the high-resolution transmission electron microscopy (HRTEM) micrograph of the SiAlN coating, indicating its amorphous structure. The SiAlN coating consists of amorphous  $\text{Si}_3\text{N}_4$  and AlN phases, where amorphous AlN phases are dispersed in the  $\text{Si}_3\text{N}_4$  matrix, as reported in our previous work [36]. Identical SiAlN coatings with a Mo interlayer were also been deposited on the ground flat surface of Ti6Al4V (shown below in Fig.8).

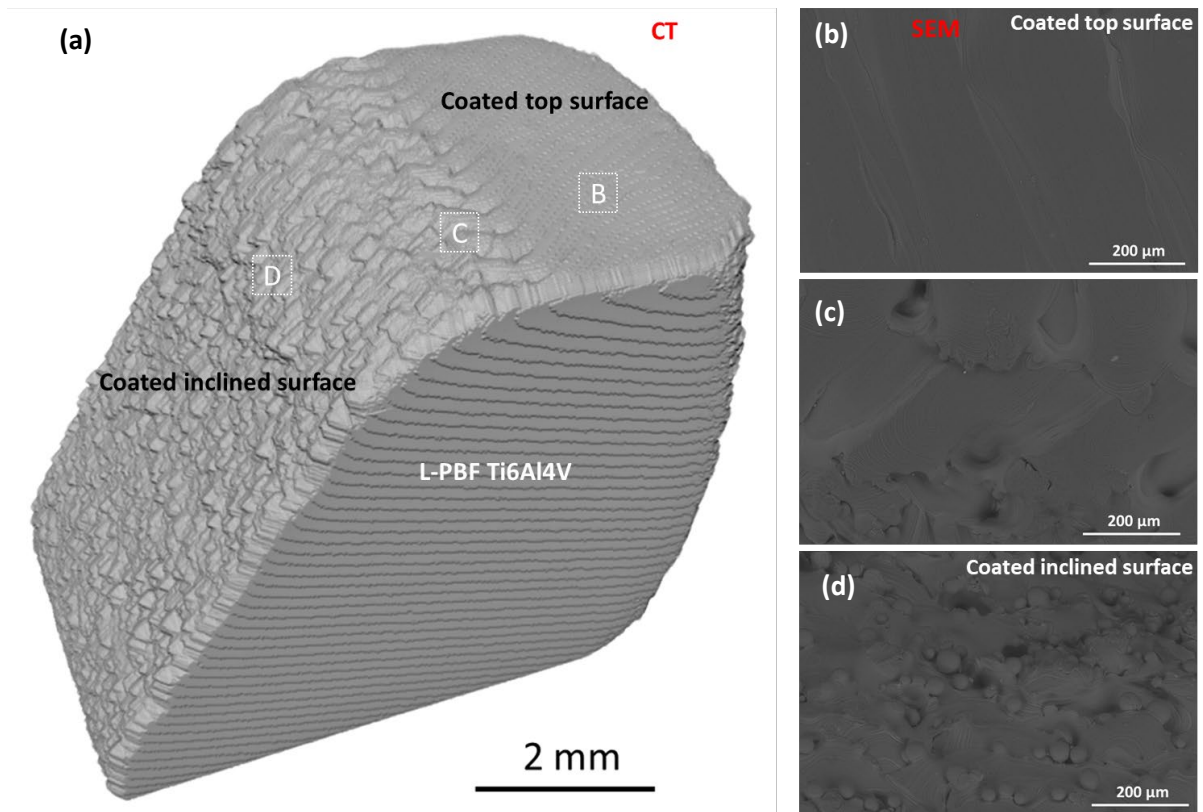


Fig.1 X-ray  $\mu$ -CT 3D volume (a) and SEM micrographs (b, c and d) of as-deposited SiAlN/Mo coating on the topographic surface of L-PBF manufactured Ti6Al4V alloy; (b), (c) and (d) acquiring from framed region B, C and D in (a), respectively.

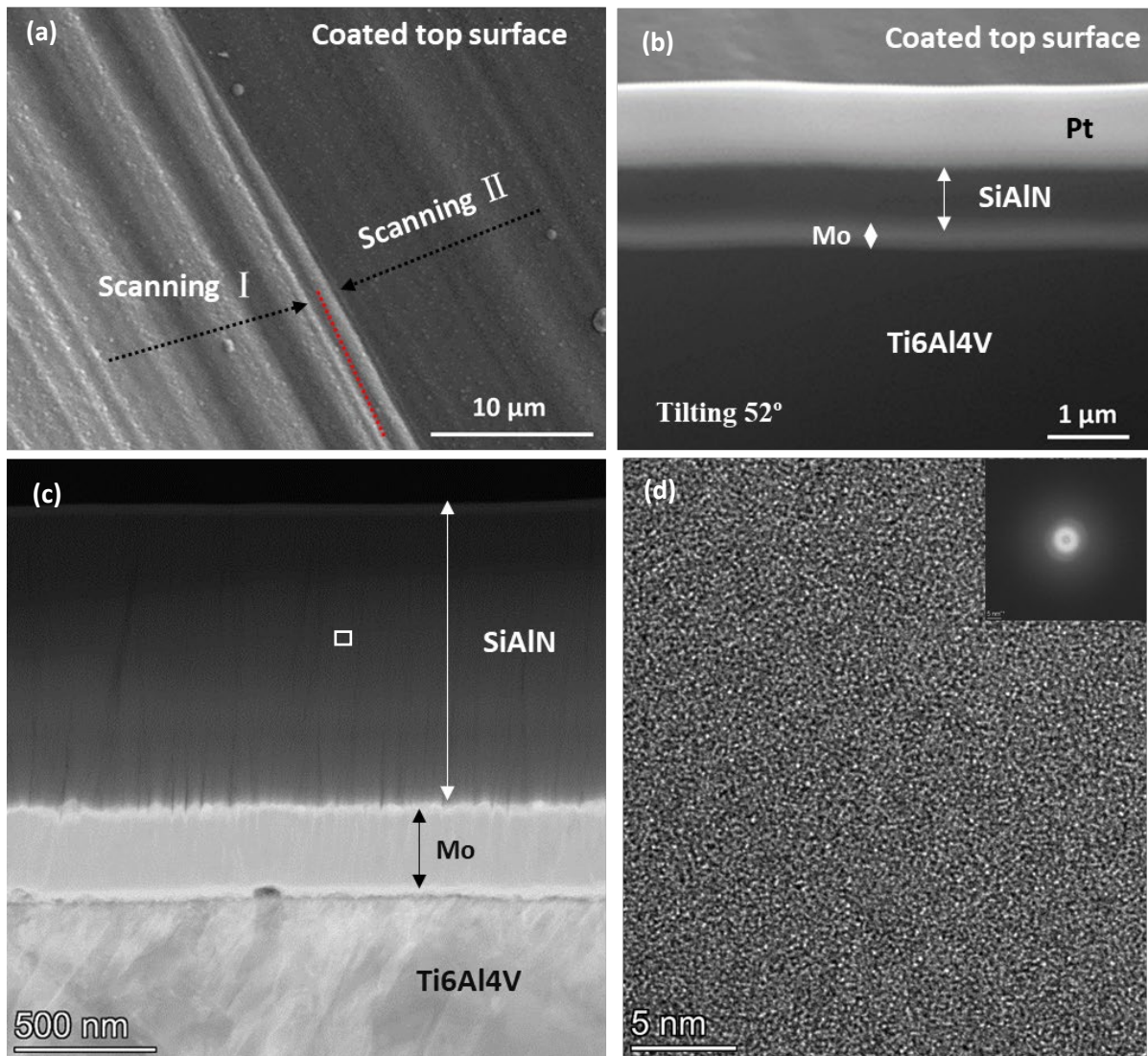


Fig.2 Top surface and cross-sectional SEM/TEM micrographs of as-deposited SiAlN/Mo coating on top topographic surface of L-PBF manufactured Ti6Al4V. (a) Top surface SEM micrograph, (b) Cross-sectional SEM micrograph, (c) Cross-sectional HAADF micrograph, (d) Cross-sectional HRTEM micrograph, acquiring from framed region in (c).

### 3.2 Oxidation behaviour in relation to surface topography

The identical SiAlN/Mo coatings deposited on the topographic surface of L-PBF manufactured Ti6Al4V and the ground flat surface of Ti6Al4V, have been thermally cycling exposed to air at 800°C to investigate whether the coating can protect the L-PBF manufactured Ti alloys against oxidation. Fig.3 shows the X-ray μ-CT 3D volume/slice and SEM micrographs of the SiAlN/Mo coating on L-PBF manufactured Ti6Al4V after oxidation at 800°C for 20 h (4 cycles). There is no coating spallation, nor any obvious cracks or observable oxidation on the top L-PBF manufactured Ti6Al4V surface covered by the SiAlN/Mo coatings, while a few locations on the coated inclined (side) surface indicate oxidation,

as shown in Fig. 3 a and b. Such phenomena can also be confirmed by the surface SEM micrographs of the SiAlN/Mo coating on L-PBF manufactured Ti6Al4V after oxidation at 800°C for 20 h (4 cycles) in Fig. 3 c and d. To examine the protection offered by the coatings in finer detail, the cross sections of the SiAlN/Mo coatings on the top topographic surface of L-PBF manufactured Ti6Al4V after thermal exposure were milled by FIB and investigated by TEM. Fig.4 shows the cross-sectional HAADF micrograph and corresponding EDS maps of this coating after oxidation at 800°C for 20 h (4 cycles). Again, it is evident that there is no observable cracking and oxidation on the coated surface. Moreover, during thermal exposure at 800°C, there is interdiffusion between the Ti substrate and Mo interlayer. The Ti can react with  $\text{Si}_3\text{N}_4$  and AlN (SiAlN consists of  $\text{Si}_3\text{N}_4$  and AlN). Thus, the as-deposited SiAlN/Mo coatings substrate interface has transformed into a complex layered structure consisting of a top remnant SiAlN layer, a new interlayer ( $\text{TiN}_{0.26}$  and  $\text{Ti}_5\text{Si}_3$ ), and a Ti-Mo solid solution layer, reported in fine detail in previous work [17]. As for the reference sample, SiAlN/Mo coated ground Ti6Al4V alloy, no coating spallation, no cracking, and no observable oxidation has been detected on the coated surface after oxidation at 800°C for 20 h (4 cycles), as shown in Fig. 5 a. Therefore, it can be expected that the SiAlN/Mo coatings can be directly deposited on the original surface of the additive manufactured Ti alloy and the coatings can provide good protection for Ti alloys against thermal exposure in the air. Such performance is better than reported  $\text{SiO}_2\text{-Al}_2\text{O}_3$ -glass,  $\text{Cr}_2\text{AlC}$  and TiAlN coatings for the protection of Ti alloy tested in static air or cyclic oxidation condition from 700°C to 900°C [17, 37-39].

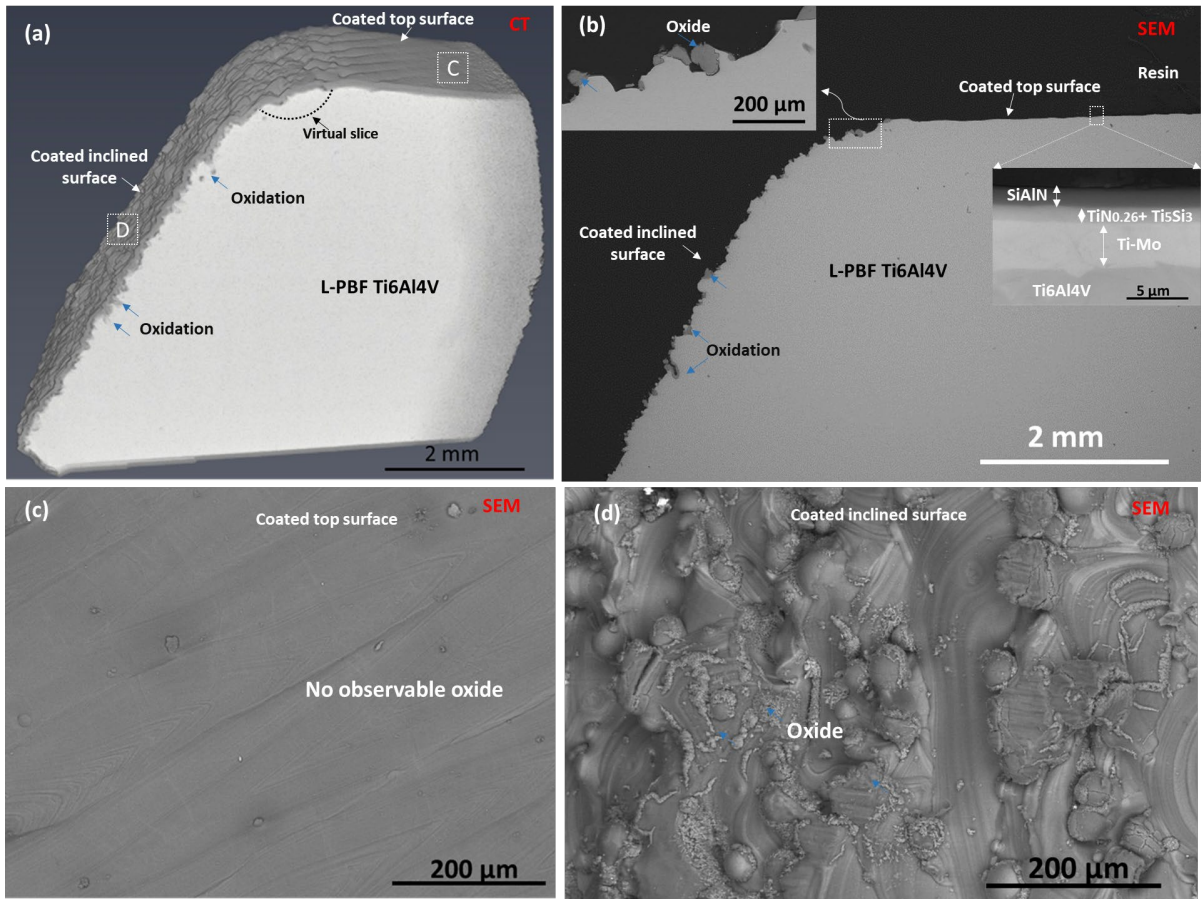


Fig.3 X-ray  $\mu$ -CT 3D volume/slice (a), cross-sectional SEM micrographs (b) and surface SEM micrographs (c and d) of SiAlN/Mo coating on L-PBF manufactured Ti6Al4V after oxidation at 800°C for 20 h (4 cycles); (c) and (d) acquiring from framed region C and D in (a), respectively.

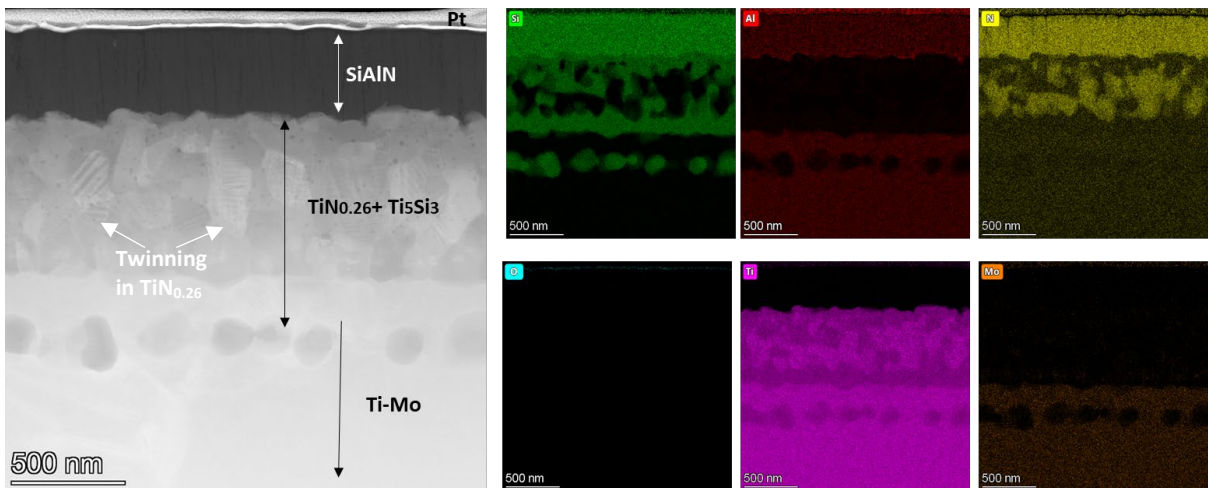


Fig.4 Cross-sectional HAADF micrograph and corresponding EDS maps of SiAlN/Mo coating on L-PBF manufactured Ti6Al4V (topographic surface) after oxidation at 800°C for 20 h (4 cycles).

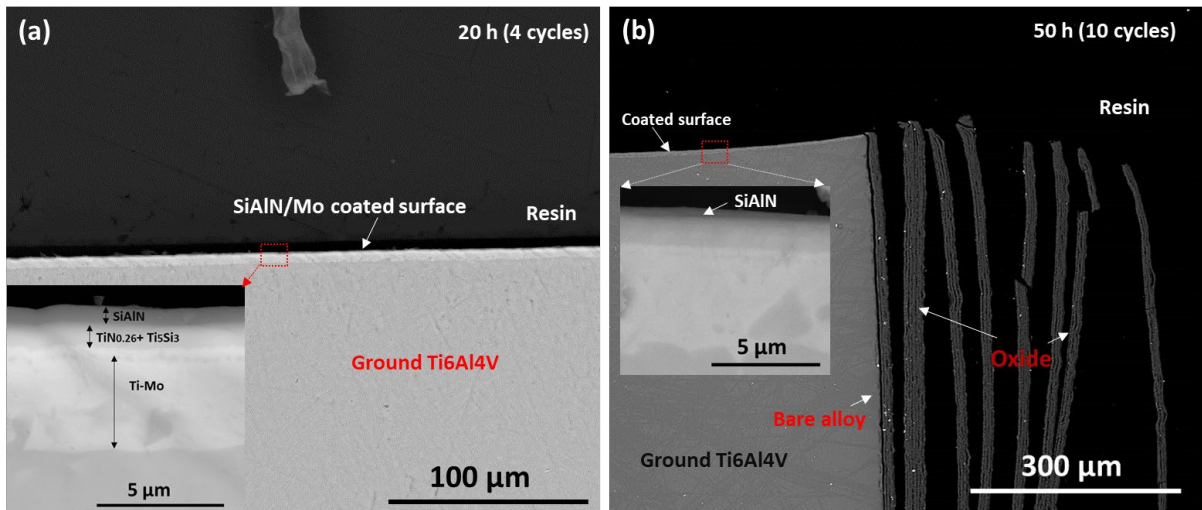


Fig.5 Cross-sectional SEM micrographs of SiAlN/Mo coating on ground Ti6Al4V (flat surface) after oxidation at 800°C for 20 h (4 cycles) (a) and 50 h (10 cycles) (b), respectively.

Extending the thermal duration from 20 h to 50 h (10 cycles), Fig.6 and Fig. 7 show X-ray  $\mu$ -CT 3D volume/slice and SEM micrographs of the SiAlN/Mo coating on L-PBF manufactured Ti6Al4V after oxidation at 800°C for 50 h (10 cycles). The SiAlN/Mo coatings still provide good protection for the top surface of the L-PBF manufactured Ti6Al4V except for a few locations along the boundaries between the adjacent laser scanning paths, where a small number of short oxide fibres have grown, as shown in Fig. 6 and Fig. 7 c/d. A large number of locations on the coated inclined surface have suffered severe oxidation, as shown in Fig.6 and 7 b. However, the coatings on the inclined surface can still provide protection to a certain extent, in comparison with the thick delaminated oxide scales on the bare alloy surfaces shown in Fig.7 a and Fig.5 b. For the SiAlN/Mo coated ground Ti6Al4V alloy, no coating spallation, no cracking, and no observable oxidation were detected after oxidation at 800°C for 50 h (10 cycles), as shown in Fig. 5 b.

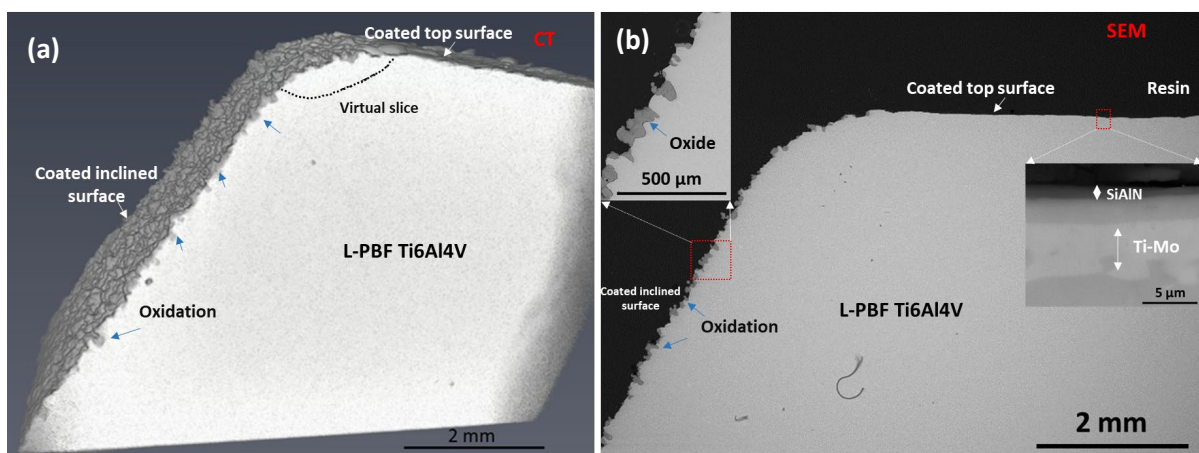


Fig.6 X-ray  $\mu$ -CT 3D volume/slice and cross-sectional SEM micrographs of SiAlN/Mo coating on L-PBF manufactured Ti6Al4V after oxidation at 800°C for 50 h (10 cycles).

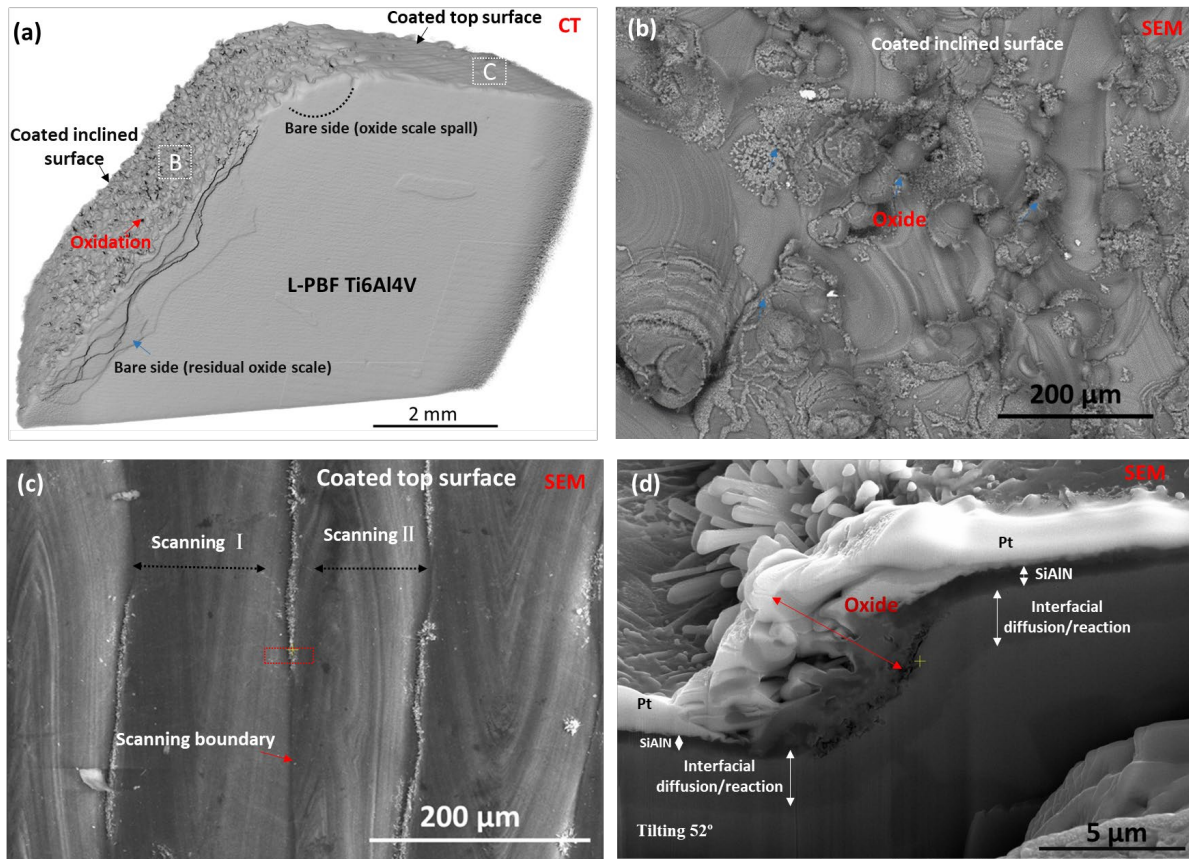


Fig.7 X-ray  $\mu$ -CT 3D volume (a) and surface SEM micrographs (b, c and d) of SiAlN/Mo coating on L-PBF manufactured Ti6Al4V after oxidation at 800°C for 50 h (10 cycles); (b) and (c) acquiring from framed region B and C in (a), respectively; (d) acquiring from framed trench region in (c).

## 4. Discussion

The findings in this work show that the identical protective SiAlN/Mo coatings deposited via magnetron sputtering not only can provide good coverage on the well-known pre-ground Ti alloys, but also directly deposited on the topographic surface of L-PBF manufactured Ti alloys without any pre-treatment. The SiAlN/Mo coatings provide good protection for both Ti alloys and the mechanistic interpretations of these findings will be explored in the following sections.

### 4.1 Coating deposition and bonding in relation to surface topography

It is well known that a protective coating design for a metallic substrate against thermal exposure at high temperature mainly consists of a top thermally stable thin film with good coating-substrate integrity (well covered, no spallation and no cracks). The pre-ground Ti6Al4V and unground, as-built L-PBF manufactured Ti6Al4V alloys have been well covered by the SiAlN/Mo coatings via magnetron sputtering. It is well known the surface topography of the substrate is an important characteristic of

PVD coatings as some topographical imperfections on the surface can cause the degradation, e.g. debonding of films [20, 21, 40]. The surface topography of a metallic substrate is mainly determined by mechanical pretreatment of the substrate and substrate ion cleaning in the sputtering chamber [20]. A mechanical pretreatment mainly consisting of grinding and polishing is widely applied to smooth the substrate surface and clean the substrate surface (oxide scale or contamination), thereby enhancing the adhesion of the film. It is rare for a metallic substrate to not receive any mechanical pretreatment before the deposition of a PVD coating. Especially, the L-PBF manufactured Ti6Al4V alloy remains a topographic surface which is rough with numerous irregularities (e.g. grooves, ridges, and spherical particles) on it. In this study, the topographic surfaces of L-PBF manufactured Ti alloys, except the lower hemisphere of the spherical particles, have been well covered by PVD coatings, confirmed by Fig.8. The length scale, or mean free path between collisions of particles (coating atoms, ions, and clusters) during sputtering enables these ejected particles to well fit a topographic surface with numerous microscale irregularities. In summary, the topographic surface has the potential to be directly utilised for PVD coating deposition.

Even though the PVD coatings have been deposited on the topographic surface, the adhesion of coatings on such a surface is the key factor in determining the performance of the coating system. The SiAlN/Mo coatings on the ground Ti6Al4V alloy have displayed good bonding and the identical coatings also strongly adhere well on the topographic surface of the L-PBF manufactured Ti6Al4V alloy even after thermal cyclic tests at high temperature (confirmed in Figs.3 to 6). The as-built (unground) L-PBF manufactured Ti6Al4V alloys were cleaned by acetone in an ultrasonic bath and have been sputter cleaned by Ar ion bombardment before the SiAlN/Mo coatings were deposited. After such cleaning processes, the unground surface of the L-PBF manufactured Ti6Al4V alloy is still expected to have a thin oxide scale as these alloys have been melted and annealed at high temperature (oxygen pick-up was 165 ppm during the L-PBF process and following vacuum annealing). The EDS O line scans of as-deposited coatings on ground Ti alloy and the topographic surface of the L-PBF manufactured Ti alloy have confirmed that a thin titanium oxide scale still exists between the L-PBF manufactured Ti alloy and the Mo interlayer coating, confirmed by Fig. 9 and illustrated in Fig. 10.

It is expected that the thin titanium oxide scale has an adverse effect on the bonding between the underlying L-PBF manufactured Ti alloys and the SiAlN/Mo coatings. However, the SiAlN/Mo coatings appear to be strongly bonded to the L-PBF manufactured Ti alloys after thermal cyclic exposure. The bonding mechanism of coatings can be simply categorized into two groups: 1) mechanical interlocking, and 2) chemical bonding [40-42]. Generally, one of the bonding mechanisms plays the dominant role. During thermal exposure at 800°C, interfacial diffusion and reactions between the underlying L-PBF manufactured Ti alloys and the SiAlN/Mo coatings have been observed in Fig.4. Interdiffusion between

Mo and Ti has been well reported [17]. But it seems Mo could also penetrate through the thin titanium oxide scale on the topographic surface of the L-PBF manufactured Ti alloys and undergo interdiffusion with Ti substrate. The refractory Mo had been reported to be very reactive towards oxygen atoms from the titanium oxide and there is diffusion of oxygen atoms into the Mo interlayer, thereby improving the interfacial bonding [43, 44]. Further extending the thermal exposure, a Mo-Ti solid solution can be rapidly formed, confirmed by the Ti-Mo diffusion zone in Fig.4, due to the high diffusivity of Mo in Ti ( $2.38 \times 10^{-14} \text{ cm}^2/\text{sec}$ , at  $800^\circ\text{C}$  [17]) and the complete solubility between Mo and Ti. Therefore, the chemical bonding dominated interface has been formed, conferring the coating enhanced adhesion.

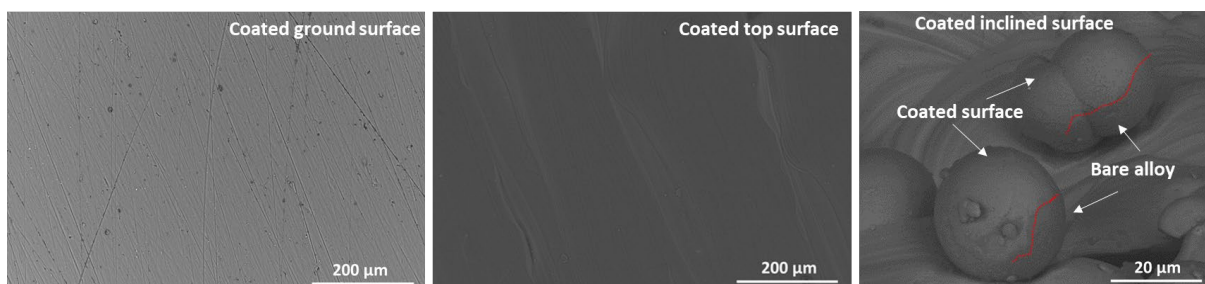


Fig.8 Top surface SEM micrographs of as-deposited SiAlN/Mo coating on ground Ti6Al4V (flat surface) and L-PBF manufactured Ti6Al4V alloys (topographic surface).

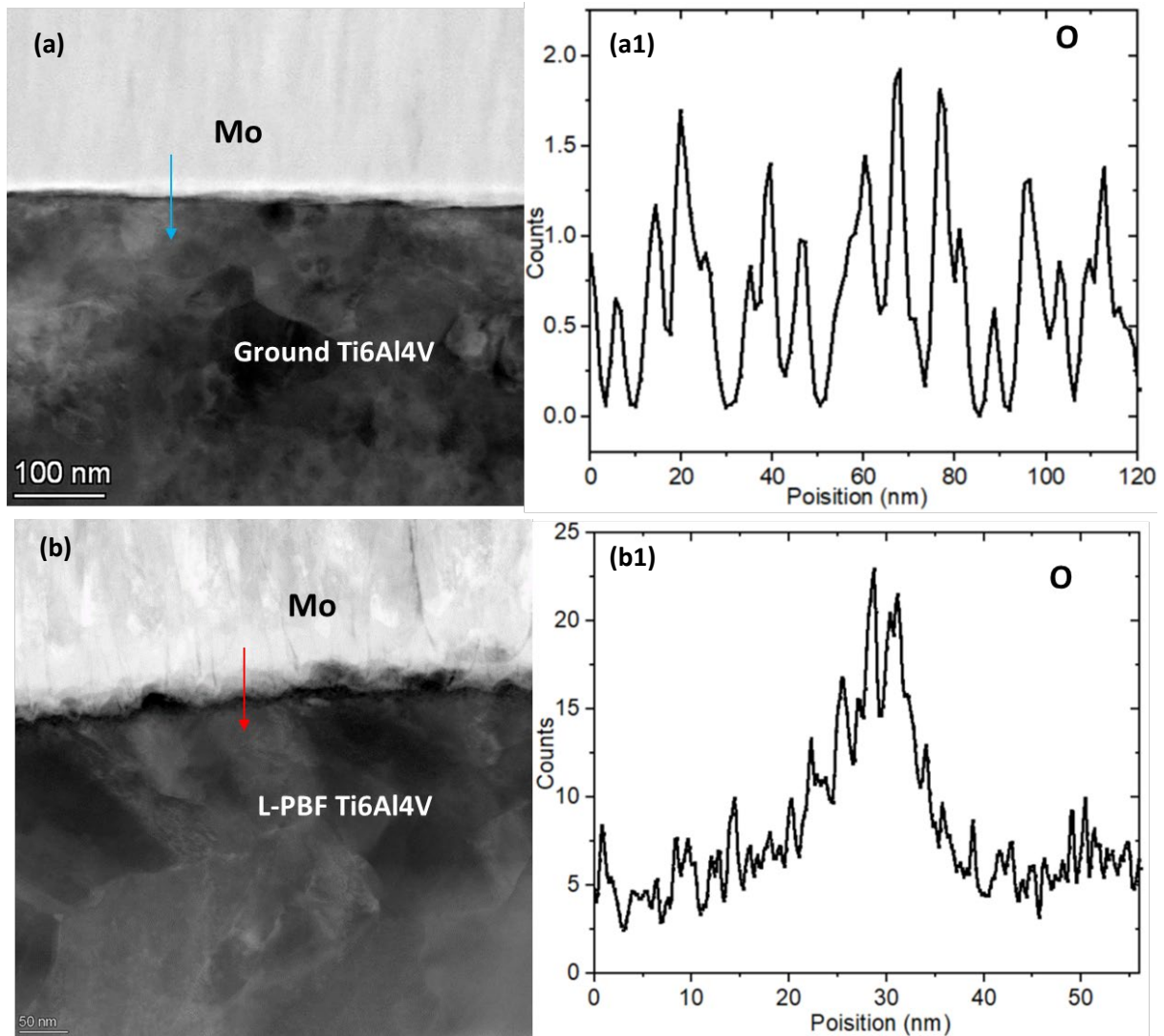


Fig.9 Cross-sectional HAADF micrographs and corresponding EDS line scans of as-deposited SiAlN/Mo coating on ground Ti6Al4V (flat surface, a and a1) and L-PBF manufactured Ti6Al4V alloys (topographic surface, b and b1).

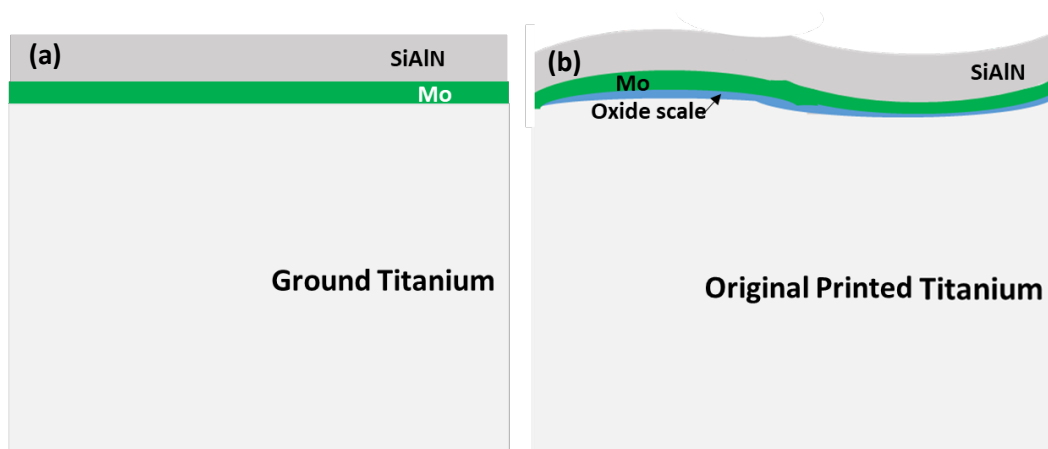


Fig.10 Schematic diagrams of as-deposited SiAlN/Mo coating on ground Ti6Al4V (flat surface) and L-PBF manufactured Ti6Al4V alloys (topographic surface).

## 4.2 Oxidation protection mechanism

The top coating, i.e., the amorphous nanocomposite SiAlN ( $\text{Si}_3\text{N}_4/\text{AlN}$ ) coating, displayed good thermal stability and excellent oxidation resistance in air at high temperatures due to its high activation energy and extremely low parabolic rate constant of oxidation [36]. As long as the SiAlN coating can provide good coverage of the Ti alloy substrates without spallation or cracking, it can provide good protection for Ti alloys against thermal cyclic exposure in the air. In this study, the SiAlN coatings provide good protection for the ground Ti alloy samples and the top topographic surface of the L-PBF manufactured Ti alloy (Figs. 3 to 6) owing to the good thermal stability of the SiAlN coating and the above discussed good coatings/substrate bonding. For the inclined (side) surface of the SLMed Ti alloy, it is largely topographic and rough even with some un-melted spherical particles on it. But the SiAlN/Mo coating can still provide protection against thermal exposure to a certain extent, as shown in Fig.11. Noticeably, the upper hemisphere of the spherical particles on the topographic surface have been well covered and protected by the SiAlN/Mo coatings, while the lower hemisphere of the spherical particles without any coatings undergo severe oxidation upon thermal cyclic exposure at 800°C in air, as shown in Fig.11 a and b. Again, this validates the hypothesis that the SiAlN/Mo coating can strongly adhere on the unground surface of the L-PBF manufactured Ti alloys and thereby provides protection for the additive manufactured Ti alloys. The gaps between the laser melted layers and the boundaries between the adjacent laser scanning in the same layer have formed oxide scales, as shown in Fig.11 a and c. The numerous pits or voids have been expected to be formed and buried in the mentioned gaps or boundaries and cannot be well covered by the PVD coating process. The SiAlN/Mo coated L-PBF manufactured Ti alloys before and after thermal exposure have been scanned by X-ray  $\mu$ -CT to track the evolution of numerous pits or voids. Fig.12 a shows the cross-sectional  $\mu$ -CT slice of the as-deposited SiAlN/Mo coating on the topographic surface of L-PBF manufactured Ti6Al4V alloy. It can be seen small numbers of pits and voids exist across the side topographic surface. Once a X-ray tomography scan of the sample in the as-deposited state had been acquired, the sample was then thermally exposed at 800°C for 20 h in air and the same region of interest was re-scanned by X-ray tomography after cooling to ambient. After this, this same sample was thermally exposed at 800°C for another 30 h (a totally 50 h) in air and was again scanned by X-ray tomography. After thermal exposure, the small numbers of pits and voids have been gradually filled with oxide material since these regions were not well covered by the protective SiAlN coatings, as shown in Fig.12 b and c respectively. Such pits or voids filled with oxide could cause the degradation of adjacent areas well coated by SiAlN/Mo, or even cause the catastrophic failure, e.g. spallation, of the topographic surface of the L-PBF manufactured Ti alloys in long term thermal exposure, especially cyclic conditions.

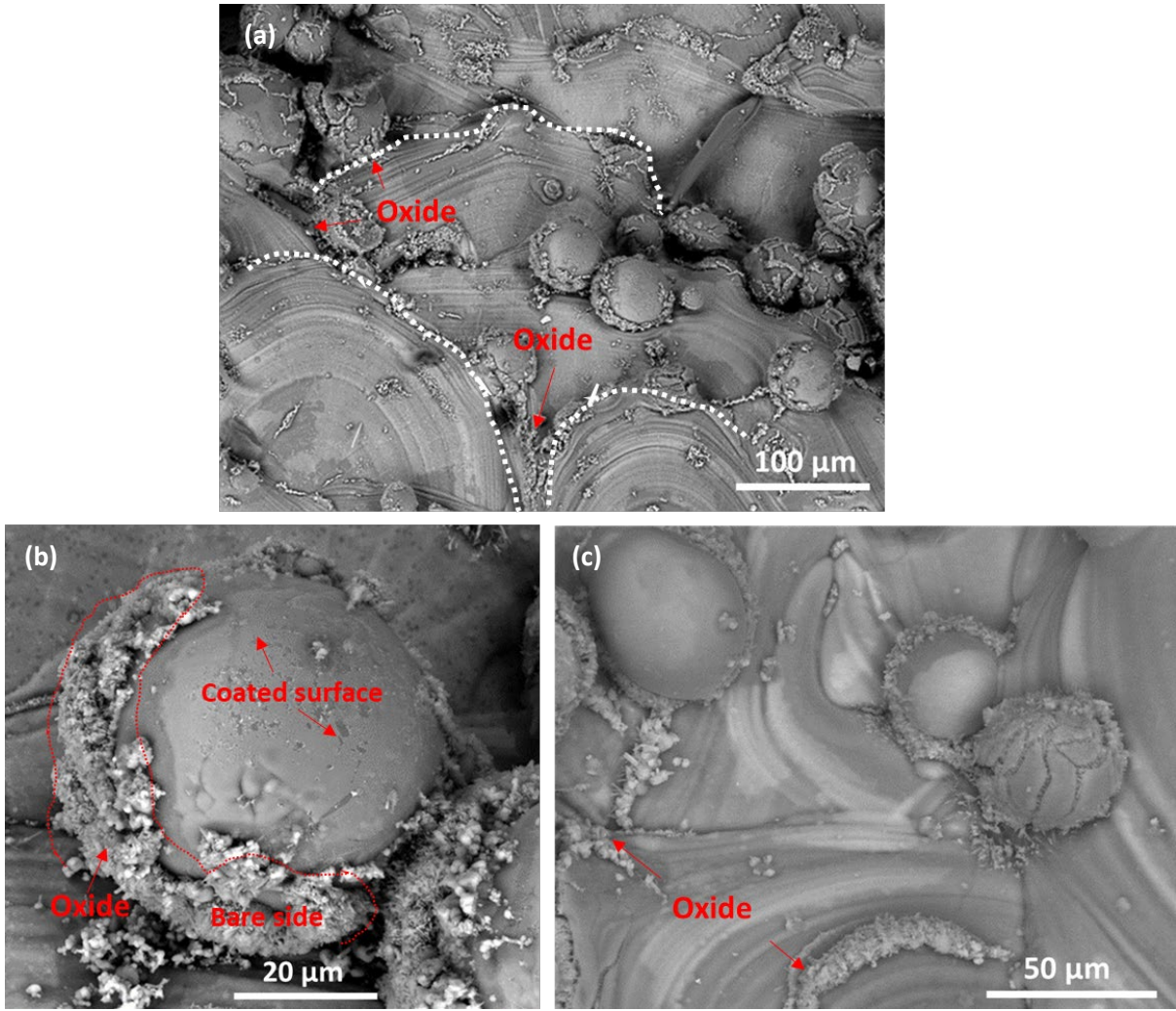


Fig.11 SEM micrographs on inclined surface of SiAlN/Mo coated L-PBF manufactured Ti6Al4V alloys after oxidation at 800°C for 20 h (4 cycles).

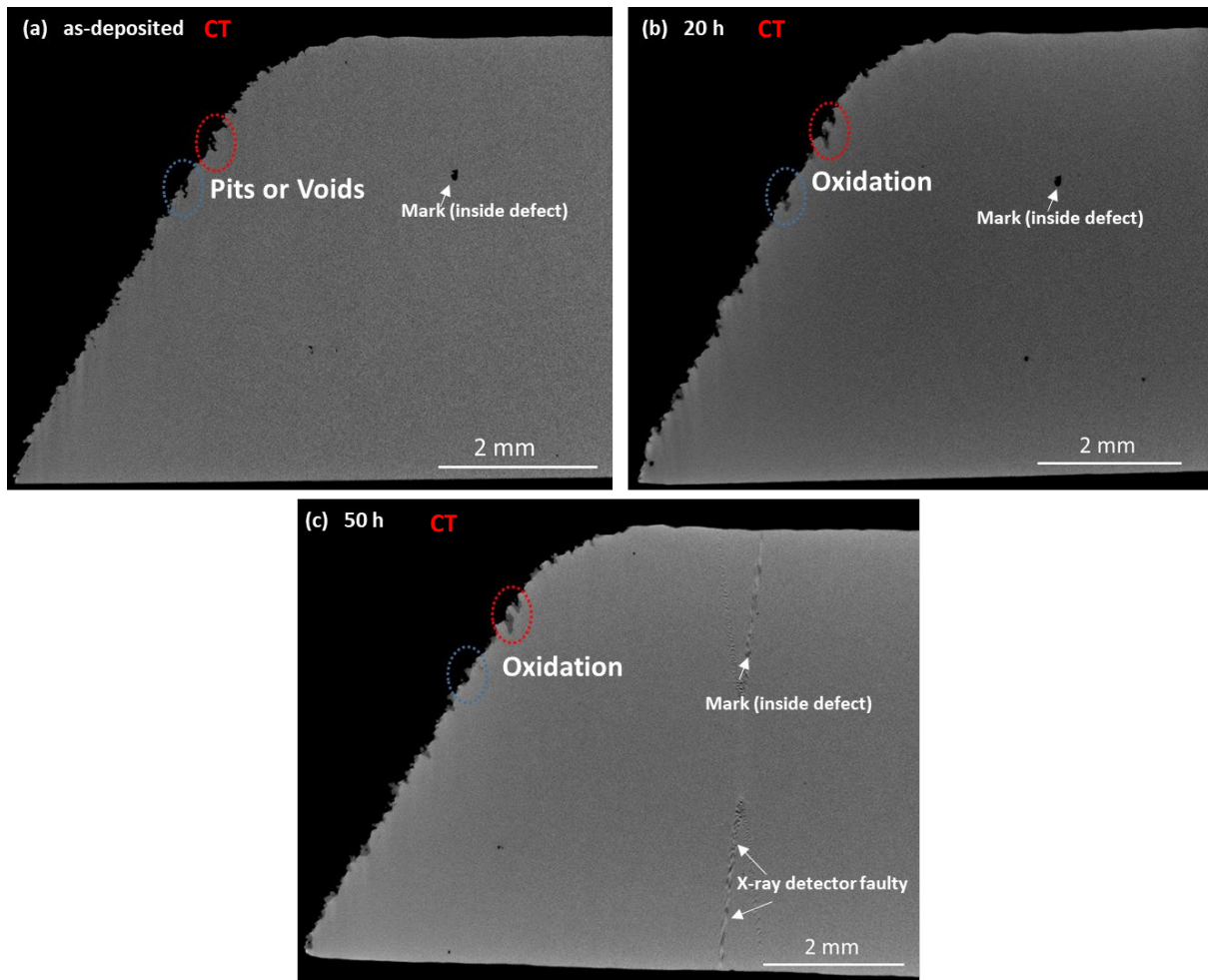


Fig.12 Cross-sectional X-ray  $\mu$ -CT virtual slices of SiAlN/Mo coated topographic surface of L-PBF manufactured Ti6Al4V alloy before and after thermal exposure. (a) as-deposited condition; (b) thermal exposure at 800°C for 20 h in air; (c) thermal exposure at 800°C for 50 h in air (isothermal treatment, samples at 20 h and 50 h are same with CT scanned as-deposited one).

## 5. Conclusion

In conclusion, a thermally stable SiAlN coating (0.9  $\mu\text{m}$  thick) with a 0.3  $\mu\text{m}$  thick Mo interlayer has been directly deposited by magnetron sputtering on the ground surface of Ti6Al4V alloy samples and the as-built topographic surface of a L-PBF manufactured Ti6Al4V alloy to serve as a protective barrier layer in high temperature harsh environments. The main conclusions are as follows:

(1) After 50 h of exposure at 800°C for 10 thermal cycles in air, the SiAlN/Mo coatings stack strongly bonds onto both the well known ground surface of the Ti alloy and the lesser studied topographic surface, even with irregular geometrical features on the L-PBF manufactured Ti6Al4V without cracking, spallation or obvious oxidation, thereby providing excellent cyclic oxidation protection.

(2) The conformal nature of the sputtered coating and the Mo diffusion through the thin native oxide scale on topographic surface into Ti alloy, enables the thermally stable SiAlN coatings to give good coverage and bond onto the surface of the L-PBF manufactured Ti alloy.

(3) The combination of PVD coating technology and the L-PBF technique enables the AMed products to be net-shape and to facilitate versatile functionality. Future work will focus on evaluating the coatings' integrity across different topographic surfaces of L-PBF alloys via adjusting printing parameters and of traditionally processed (rolled or extruded) alloys, and the corresponding degradation mechanism of coatings and the theoretical modelling of their connection will also be covered.

## Acknowledgment

PX would like to acknowledge support from Royal Academy of Engineering and Rolls-Royce for appointment of Rolls-Royce/Royal Academy of Engineering Research Chair in Advanced Coating Technology. The authors also thank National X-ray Computed Tomography (NXCT) for beamtimes and for imaging processing and support.

## References

- [1] A. Devaraj, V.V. Joshi, A. Srivastava, S. Manandhar, V. Moxson, V.A. Duz, C. Lavender, A low-cost hierarchical nanostructured beta-titanium alloy with high strength, *Nat. Commun.* 7 (2016) 11176.
- [2] S.H. Z. Wang, H. Lu, J. Liu, I. Alexandrov, K. Luo, J. Lu, The role of annealing heat treatment in high-temperature oxidation resistance of laser powder bed fused Ti6Al4V alloy subjected to massive laser shock peening treatment, *Corros. Sci.* 209 (2022) 110732.
- [3] L.C. Y. Cui, P. Qin, R. Li, Q. Zang, J. Peng, L. Zhang, S. Lu, L. Wang, L. Zhang, Metastable pitting corrosion behavior of laser powder bed fusion produced Ti-6Al-4V in Hank's solution, *Corros. Sci.* 203 (2022) 110333.
- [4] Z. Lin, K. Song, X. Yu, A review on wire and arc additive manufacturing of titanium alloy, *J. Manuf. Process.* 70 (2021) 24-45.
- [5] C. de Formanoir, G. Martin, F. Prima, S.Y.P. Allain, T. Dessolier, F. Sun, S. Vivès, B. Hary, Y. Bréchet, S. Godet, Micromechanical behavior and thermal stability of a dual-phase  $\alpha+\alpha'$  titanium alloy produced by additive manufacturing, *Acta Mater.* 162 (2019) 149-162.
- [6] T. Grover, A. Pandey, S.T. Kumari, A. Awasthi, B. Singh, P. Dixit, P. Singhal, K.K. Saxena, Role of titanium in bio-implants and additive manufacturing: An overview, *Mater. Today: Proc.* 26 (2020) 3071-3080.
- [7] S. Pal, G. Lojen, R. Hudak, V. Rajtukova, T. Brajljih, V. Kokol, I. Drstvenšek, As-fabricated surface morphologies of Ti-6Al-4V samples fabricated by different laser processing parameters in selective laser melting, *Addit. Manuf.* 33 (2020) 101147.

- [8] M. McGregor, S. Patel, S. McLachlin, V. Mihaela, Architectural bone parameters and the relationship to titanium lattice design for powder bed fusion additive manufacturing, *Addit. Manuf.* 47 (2021) 102273.
- [9] D. Sharma, S.R. Kada, D. Fabijanic, D. Parfitt, B. Chen, B. Roebuck, M.E. Fitzpatrick, M.R. Barnett, The ageing response of direct laser deposited metastable  $\beta$ -Ti alloy, Ti-5Al-5Mo-5V-3Cr, *Addit. Manuf.* 48 (2021) 102384.
- [10] C.F. Tey, X. Tan, S.L. Sing, W.Y. Yeong, Additive manufacturing of multiple materials by selective laser melting: Ti-alloy to stainless steel via a Cu-alloy interlayer, *Addit. Manuf.* 31 (2020) 100970.
- [11] W.E. Frazier, Metal Additive Manufacturing: A Review, *J. Mater. Eng. Perform.* 23(6) (2014) 1917-1928.
- [12] Z.H. Tianlong Zhang, Tao Yang, Haojie Kong, Junhua Luan, Anding Wang, W.K. Dong Wang, Yunzhi Wang, Chain-Tsuan Liu, In situ design of advanced titanium alloy with concentration modulations by additive manufacturing, *Science* 374 (2021) 478-482.
- [13] Z. Chen, X. Wu, D. Tomus, C.H.J. Davies, Surface roughness of Selective Laser Melted Ti-6Al-4V alloy components, *Addit. Manuf.* 21 (2018) 91-103.
- [14] A. Khorasani, I. Gibson, U.S. Awan, A. Ghaderi, The effect of SLM process parameters on density, hardness, tensile strength and surface quality of Ti-6Al-4V, *Addit. Manuf.* 25 (2019) 176-186.
- [15] M.H. Nasab, D. Gastaldi, N.F. Lecis, M. Vedani, On morphological surface features of the parts printed by selective laser melting (SLM), *Addit. Manuf.* 24 (2018) 373-377.
- [16] T. Majumdar, N. Eisenstein, J.E. Frith, S.C. Cox, N. Birbilis, Additive Manufacturing of Titanium Alloys for Orthopedic Applications: A Materials Science Viewpoint, *Adv. Eng. Mater.* 20(9) (2018) 1800172.
- [17] Z. Gao, Z. Zhang, X. Zhang, J. Kulczyk-Malecka, H. Liu, P. Kelly, P.J. Withers, P. Xiao, A conformable high temperature nitride coating for Ti alloys, *Acta Mater.* 189 (2020) 274-283.
- [18] J. Musil, Hard nanocomposite coatings: Thermal stability, oxidation resistance and toughness, *Surf. Coat. Technol.* 207 (2012) 50-65.
- [19] J. Musil, J. Vlček, P. Zeman, Hard amorphous nanocomposite coatings with oxidation resistance above 1000°C, *Adv. Appl. Ceram.* 107(3) (2013) 148-154.
- [20] P. Panjan, A. Drnovšek, P. Gselman, M. Čekada, M. Panjan, Review of Growth Defects in Thin Films Prepared by PVD Techniques, *Coatings* 10(5) (2020).
- [21] A. Guzanová, J. Brezinová, D. Draganovská, F. Jaš, A study of the effect of surface pre-treatment on the adhesion of coatings, *J. Adhes. Sci. Technol.* 28(17) (2014) 1754-1771.
- [22] B. Vayssette, N. Saintier, C. Brugger, M. El May, E. Pessard, Numerical modelling of surface roughness effect on the fatigue behavior of Ti-6Al-4V obtained by additive manufacturing, *Int. J. Fatigue* 123 (2019) 180-195.
- [23] A. Balyakin, E. Goncharov, E. Zhuchenko, The effect of preprocessing on surface quality in the chemical polishing of parts from titanium alloy produced by SLM, *Mater. Today: Proc.* 19 (2019) 2291-2294.
- [24] A. Polishetty, M. Shunmugavel, M. Goldberg, G. Littlefair, R.K. Singh, Cutting Force and Surface Finish Analysis of Machining Additive Manufactured Titanium Alloy Ti-6Al-4V, *Procedia Manuf.* 7 (2017) 284-289.

- [25] R. Bertolini, L. Lizzul, L. Pezzato, A. Ghiotti, S. Bruschi, Improving surface integrity and corrosion resistance of additive manufactured Ti6Al4V alloy by cryogenic machining, *Int. J. Adv. Manuf.* 104(5-8) (2019) 2839-2850.
- [26] C.L.A. Leung, S. Marussi, R.C. Atwood, M. Towrie, P.J. Withers, P.D. Lee, In situ X-ray imaging of defect and molten pool dynamics in laser additive manufacturing, *Nat. Commun.* 9(1) (2018) 1355.
- [27] Y. Huang, T.G. Fleming, S.J. Clark, S. Marussi, K. Fezzaa, J. Thiyagalingam, C.L.A. Leung, P.D. Lee, Keyhole fluctuation and pore formation mechanisms during laser powder bed fusion additive manufacturing, *Nat. Commun.* 13(1) (2022) 1170.
- [28] J. Günther, S. Leuders, P. Koppa, T. Tröster, S. Henkel, H. Biermann, T. Niendorf, On the effect of internal channels and surface roughness on the high-cycle fatigue performance of Ti-6Al-4V processed by SLM, *Mater. Des.* 143 (2018) 1-11.
- [29] L.-C. Zhang, H. Attar, Selective laser melting of titanium alloys and titanium matrix composites for biomedical applications: A review, *Adv. Eng. Mater.* 18(4) (2016) 463-475.
- [30] Y. Sato, M. Tsukamoto, Y. Yamashita, Surface morphology of Ti-6Al-4V plate fabricated by vacuum selective laser melting, *Appl. Phys. B* 119(3) (2015) 545-549.
- [31] M. Jamshidinia, R. Kovacevic, The influence of heat accumulation on the surface roughness in powder-bed additive manufacturing, *Surf. Topogr.* 3(1) (2015).
- [32] D. Wang, S. Wu, F. Fu, S. Mai, Y. Yang, Y. Liu, C. Song, Mechanisms and characteristics of spatter generation in SLM processing and its effect on the properties, *Mater. Des.* 117 (2017) 121-130.
- [33] D. Dai, D. Gu, Tailoring surface quality through mass and momentum transfer modeling using a volume of fluid method in selective laser melting of TiC/AlSi10Mg powder, *Int. J. Mach. Tools Manuf.* 88 (2015) 95-107.
- [34] K. Mumtaz, N. Hopkinson, Top surface and side roughness of Inconel 625 parts processed using selective laser melting, *Rapid Prototyp. J.* 15(2) (2009) 96-103.
- [35] S. Cao, R. Chu, X. Zhou, K. Yang, Q. Jia, C.V.S. Lim, A. Huang, X. Wu, Role of martensite decomposition in tensile properties of selective laser melted Ti-6Al-4V, *J. Alloys Compd.* 744 (2018) 357-363.
- [36] Z. Gao, J. Kulczyk-Malecka, Z. Zhang, H. Liu, X. Zhang, Y. Chen, P. Hill, P. Kelly, P. Xiao, Oxidation and degradation of amorphous SiAlN coating via forming Si-Si bond, *Corros. Sci.* 183 (2021).
- [37] W. Li, S. Zhu, C. Wang, M. Chen, M. Shen, F. Wang, SiO<sub>2</sub>-Al<sub>2</sub>O<sub>3</sub>-glass composite coating on Ti-6Al-4V alloy: Oxidation and interfacial reaction behavior, *Corros. Sci.* 74 (2013) 367-378.
- [38] Q.M. Wang, A. Flores Renteria, O. Schroeter, R. Mykhaylonka, C. Leyens, W. Garkas, M. to Baben, Fabrication and oxidation behavior of Cr<sub>2</sub>AlC coating on Ti6242 alloy, *Surf. Coat. Technol.* 204(15) (2010) 2343-2352.
- [39] M. Zhang, Y. Cheng, L. Xin, J. Su, Y. Li, S. Zhu, F. Wang, Cyclic oxidation behaviour of Ti/TiAlN composite multilayer coatings deposited on titanium alloy, *Corros. Sci.* 166 (2020).
- [40] B. Ramamoorthy, An Investigation into the Adhesion Strength of Diamond Like Carbon Multilayer Coating (DLC/TiN/Ti/Cu/Ni), *Intell. Inf. Manag.* 01(03) (2009) 179-194.
- [41] H. Weiss, Adhesion of advanced overlay coatings mechanisms and quantitative, *Surf. Coat. Technol.* 71 (1995) 201-207.

[42] M. Arif Butt, Arshad Chughtai, Javaid Ahmad, Rafiq Ahmad, Usman Majeed, I.H. Khan, Theory of adhesion and its practical implications, Journal of Faculty of Engineering & Technology (2007-2008) 21-45.

[43] B. Domenichini, S. Pe'tigny, V. Blondeau-Patissier, A. Steinbrunn, S. Bourgeois, Effect of the surface stoichiometry on the interaction of Mo with TiO<sub>2</sub> (110), Surf. Sci. 468 (2000) 192-202.

[44] B. Domenichini, M. Petukhov, G.A. Rizzi, M. Sambì, S. Bourgeois, G. Granozzi, Epitaxial growth of molybdenum on TiO<sub>2</sub>(110), Surf. Sci. 544(2-3) (2003) 135-146.